

A single hole spin with enhanced coherence in natural silicon

N. Piot,^{1,*} B. Brun,^{1,*} V. Schmitt,¹ S. Zihlmann,¹ V. P. Michal,² A. Apra,¹ J. C. Abadillo-Uriel,² X. Jehl,¹ B. Bertrand,³ H. Niebojewski,³ L. Hutin,³ M. Vinet,³ M. Urdampilleta,⁴ T. Meunier,⁴ Y.-M. Niquet,² R. Maurand,^{1,†} and S. De Franceschi^{1,‡}

¹*Univ. Grenoble Alpes, CEA, Grenoble INP, IRIG-Pheliqs, Grenoble, France.*

²*Univ. Grenoble Alpes, CEA, Grenoble INP, IRIG-MEM-L-Sim, Grenoble, France.*

³*Univ. Grenoble Alpes, CEA, LETI, Minatec Campus, Grenoble, France.*

⁴*Univ. Grenoble Alpes, CNRS, Grenoble INP, Institut Néel, Grenoble, France.*

(Dated: January 24, 2022)

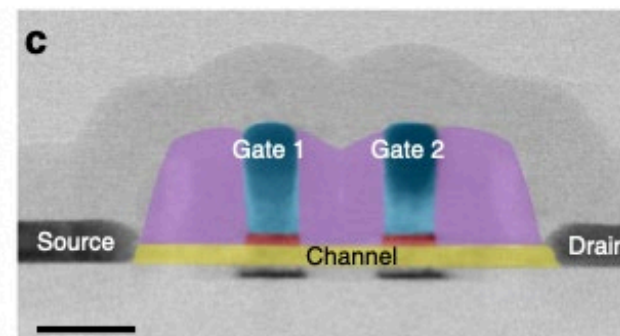
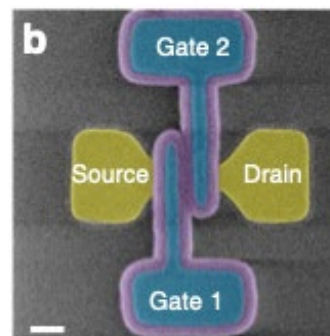
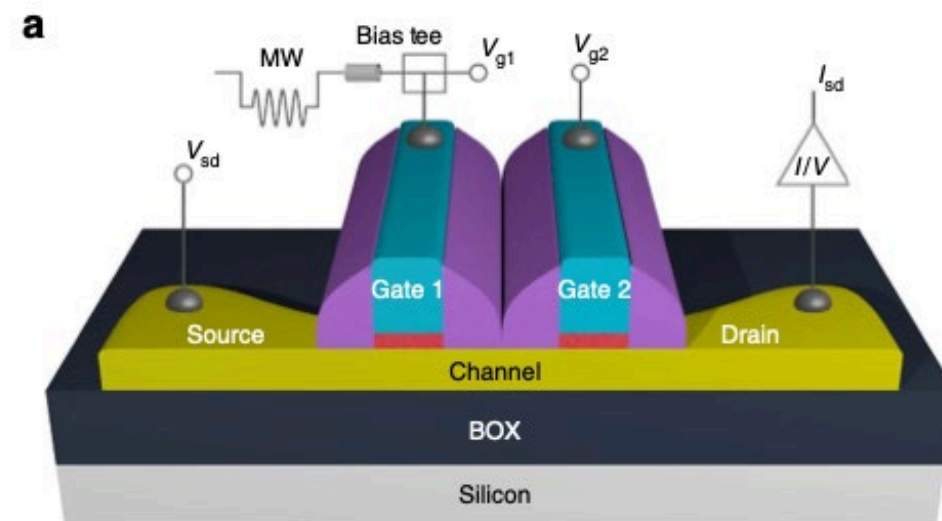
<https://arxiv.org/pdf/2201.08637.pdf>

Journal club 31.01.2022

Nico Hendrickx

LETI devices

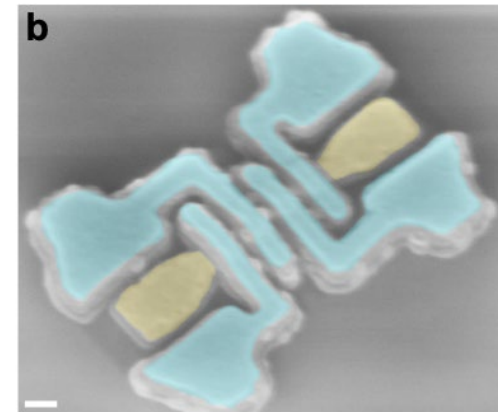
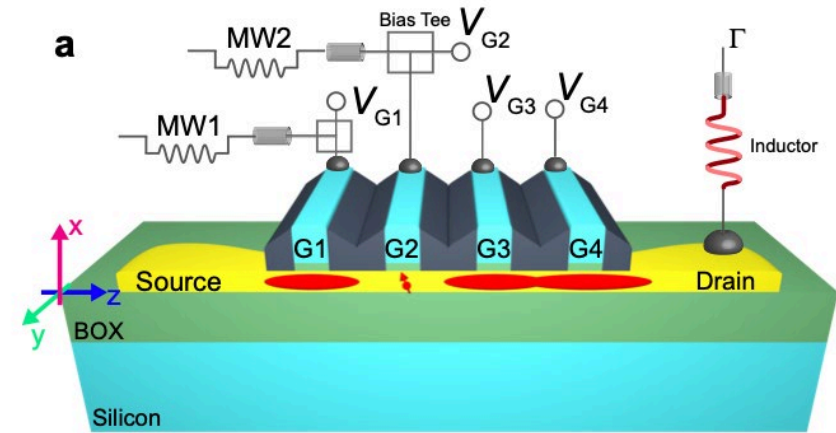
- Silicon finFET devices
- SOI fin
- Transport qubits in 2016
- Optical + ebpq
- LETI/Copenhagen/UCL/EPFL



Maurand et al. Nat. Comm. 13575 (2016)
<https://www.nature.com/articles/ncomms13575.pdf>

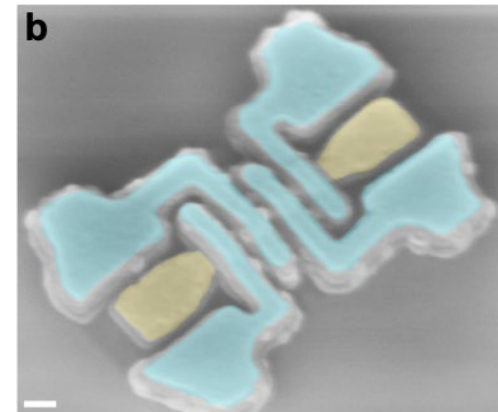
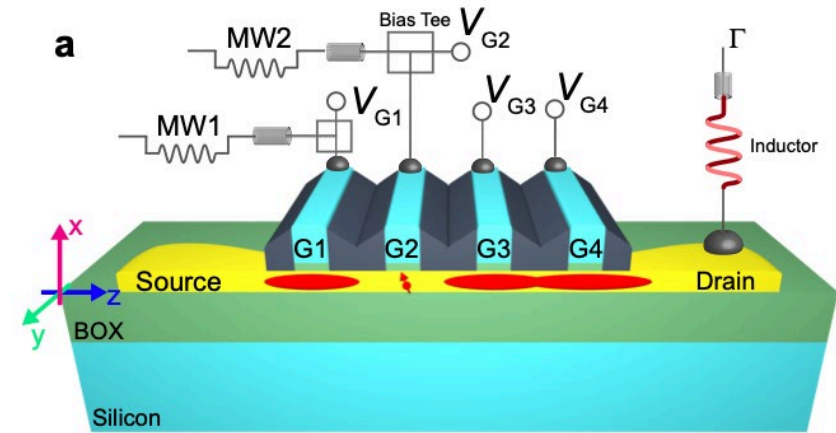
Device design (fig. 1a-b)

- Gate stack:
 - Metal topgate
 - 250 nm SiO₂
 - 35 nm Si₃N₄ (etch stop)
 - 50 nm polySi
 - 6 nm TiN
 - 6 nm SiO₂
 - Natural Si fin
 - BOX
 - Doped Si (back gate)



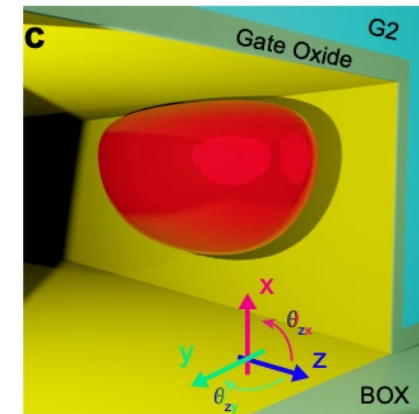
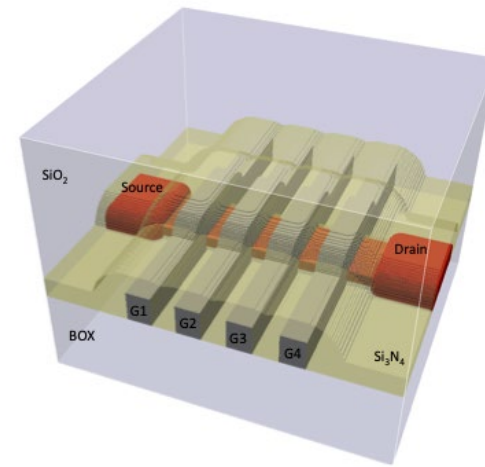
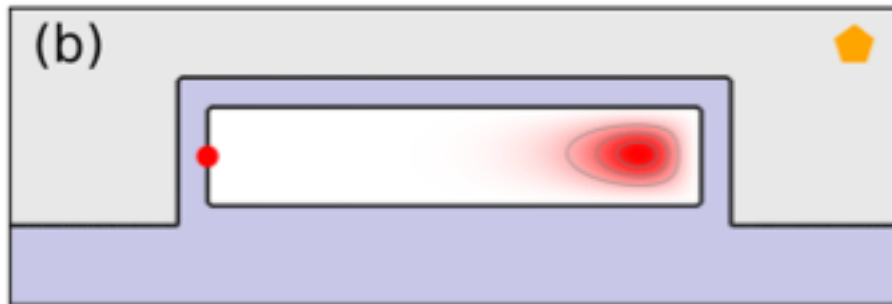
Device design (fig. 1a-b)

- Four gate device
 - G₃/G₄ large dot (sensor)
 - G₁ dot to screen S (no mention of effect)
 - Scalebar = 100 nm



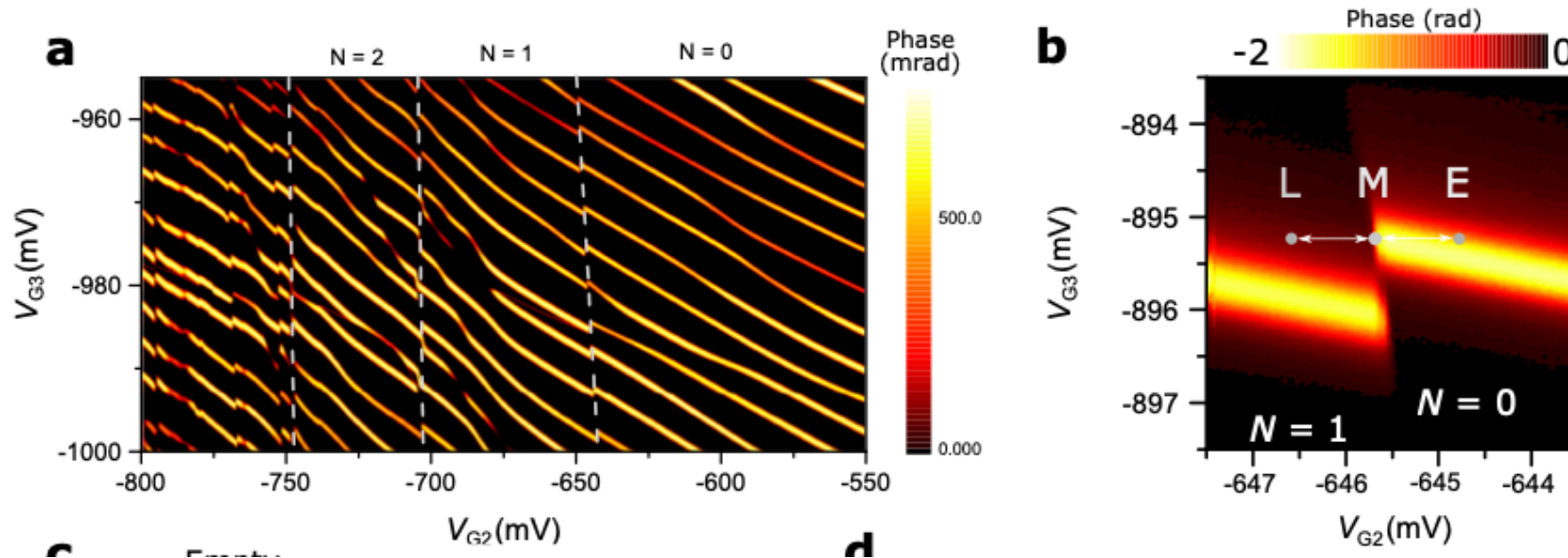
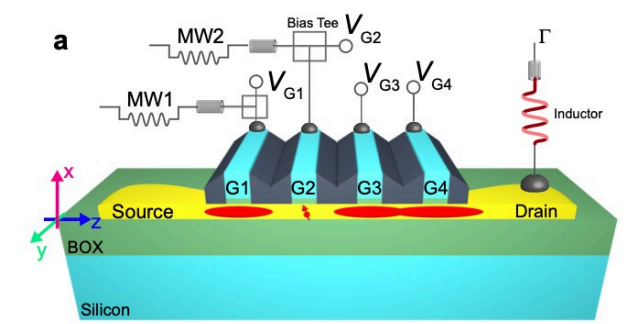
Dot accumulation (fig. S2 / S4b)

- Poisson solver
 - Two corner dots are preferred
 - E-field is stronger
- Assume: degeneracy due to disorder
 - Result: only a single corner dot
 - Strong intermixing of LH/HH states



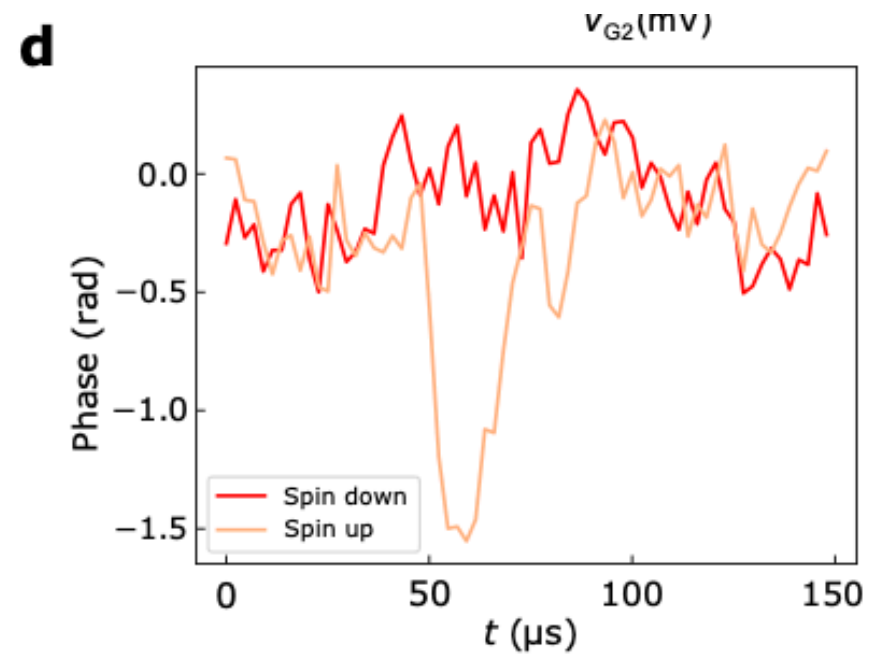
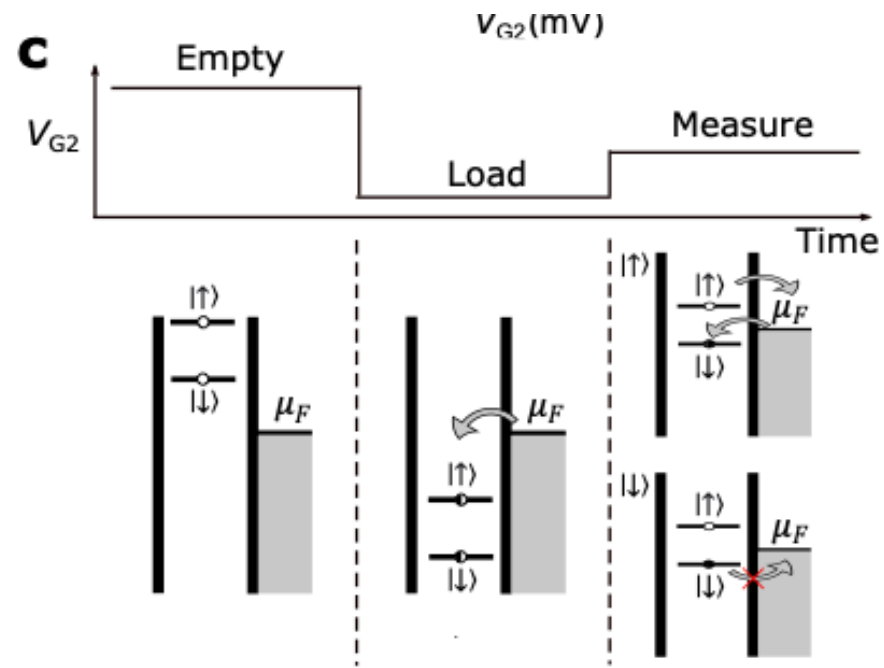
Charge stability diagram (fig. S1)

- Off-the-shelve resonator connected to drain.
- $D \leftrightarrow G_3/G_4$ dot transitions as sensor

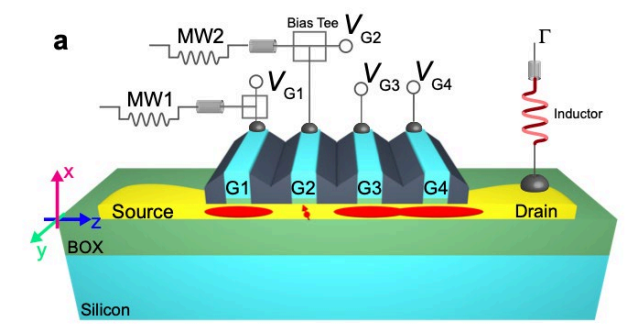


Spin readout (fig. S1)

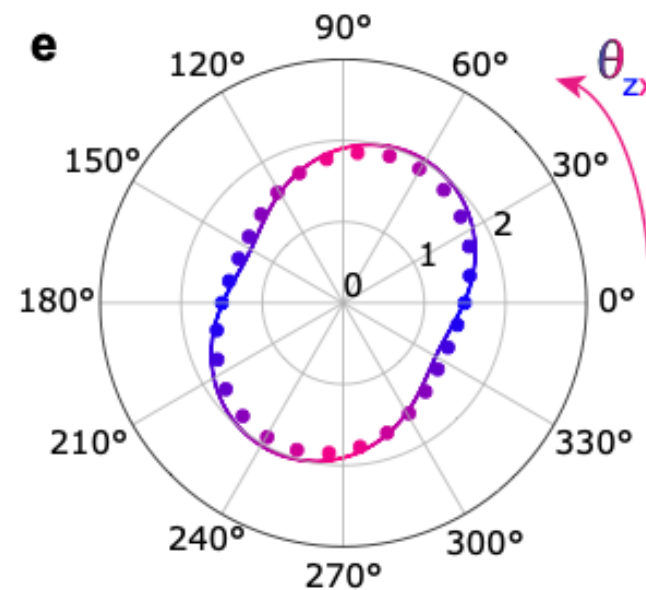
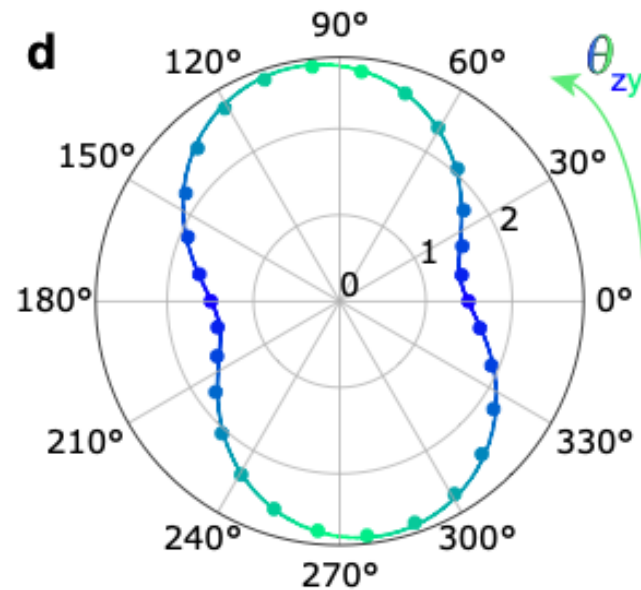
- Elzerman readout



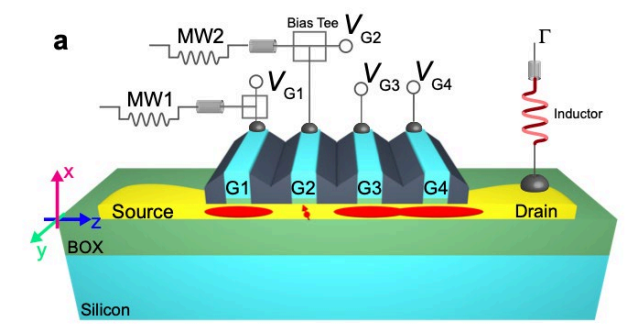
g-factor measurement (fig. 1d/e)



- Measure resonance frequency a.f.o. field orientation ($B = ??$)
- Not very anisotropic
- No XY data (1 axis of their vector magnet broken ...)



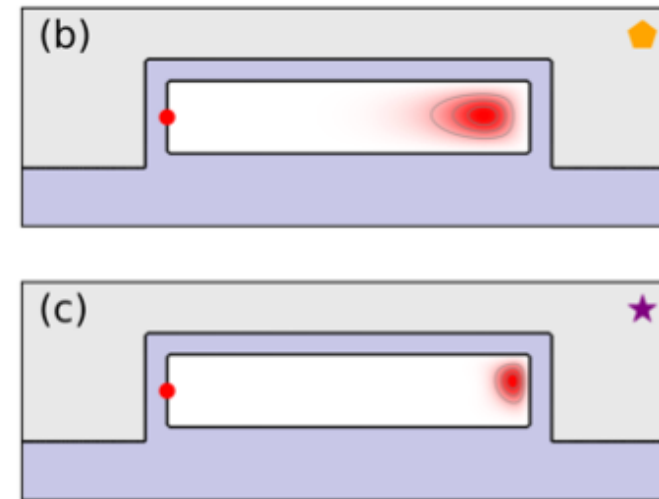
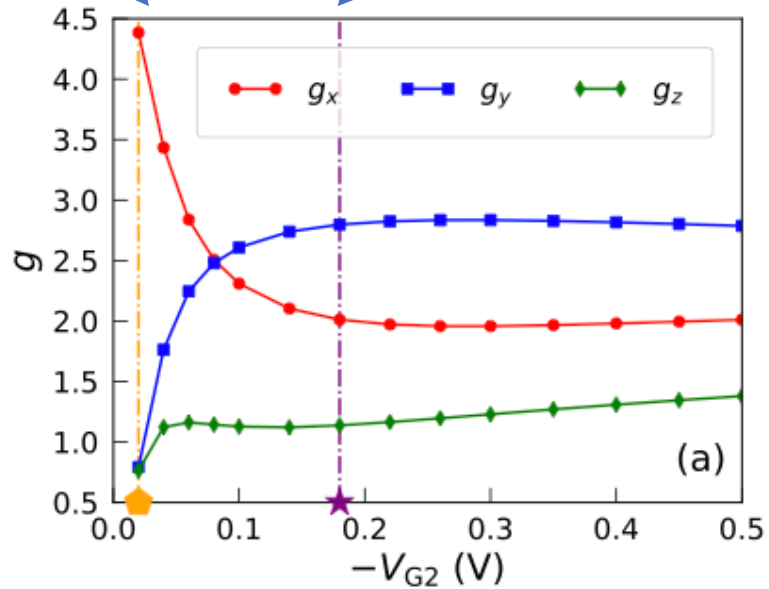
g-factor measurement (fig. 1d/e)



- Not very anisotropic
 - Result of the strong HH/LH mixing (due to lateral fields)

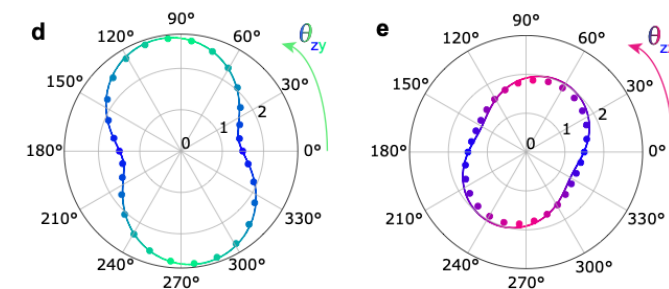
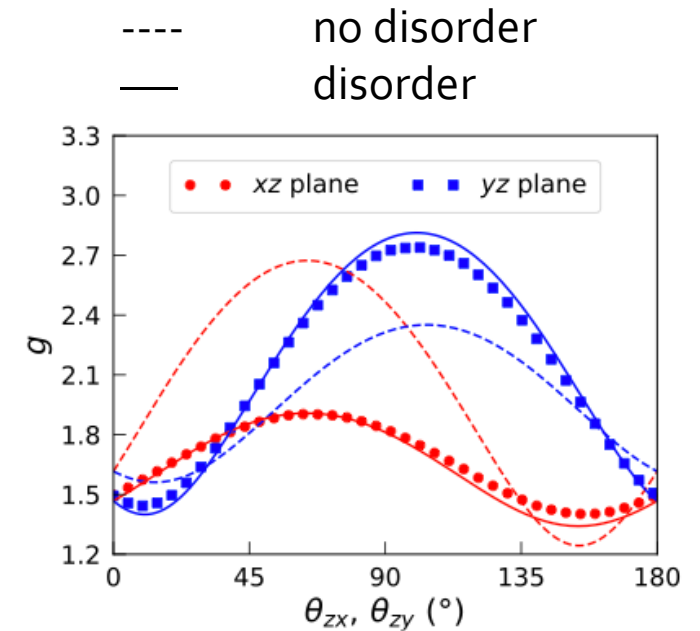
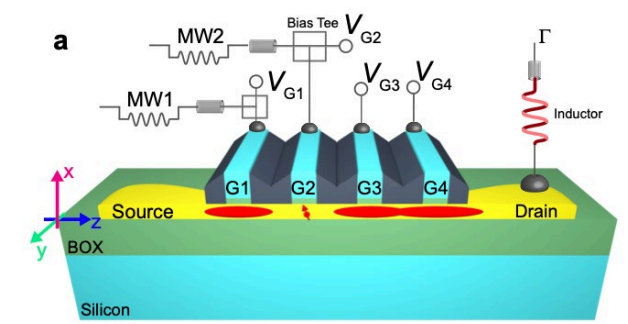
Dominant E_x
more 'planar'
purer HH

$E_x + E_y$
more 'corner'
mixed LH/HH

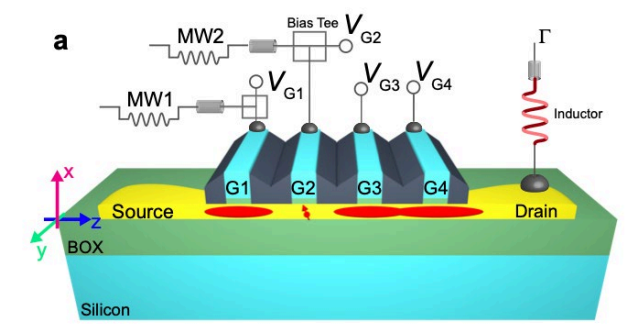


g-factor fit (fig. S5)

- Rotational shift
 - 35 deg shift in ZX
 - 10 deg shift in ZY
 - In modelling: assume B-field misalignment
 - Hypothesis is cool down strain (but polySi gates ?)
 - shear strain: 0.1 %
- Discrepancy in size
 - Disorder
 - σ_{trap} at Si/SiO₂ interface
 - ρ_{trap} in Si₃N₄ spacer



E-field dependence of Larmor frequency (fig. 2)



- They coin the term LSES: Longitudinal spin-electric susceptibility

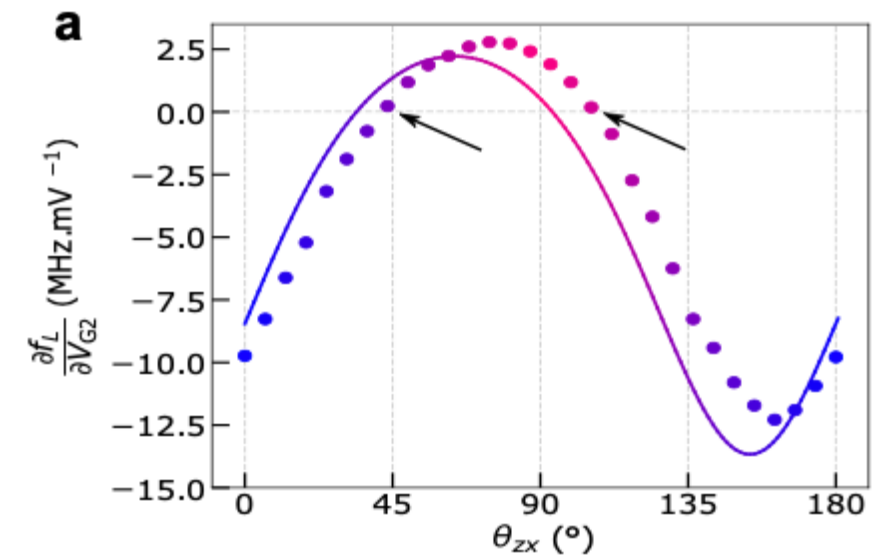
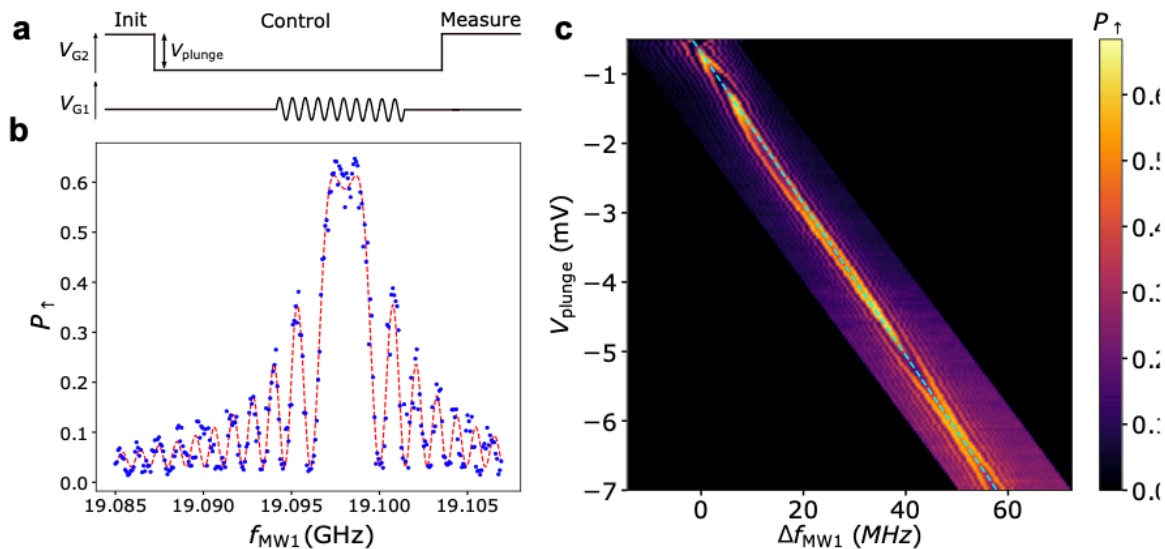
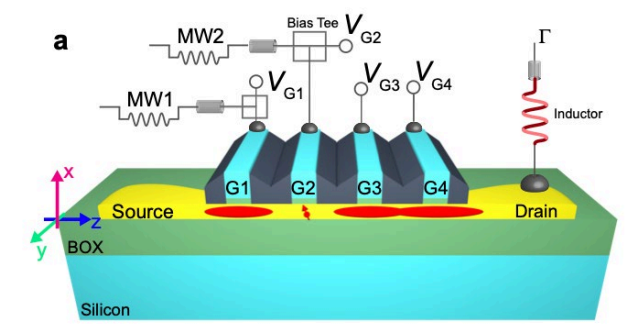
- i.e. $LSES = \frac{\delta f_q}{\delta V_{gate}}$

- Assumptions:

- G1 purely parallel
 - G2 purely perpendicular
 - But also: *"Note that the action of V_{G1} is strongly screened by the hole gas beneath"*

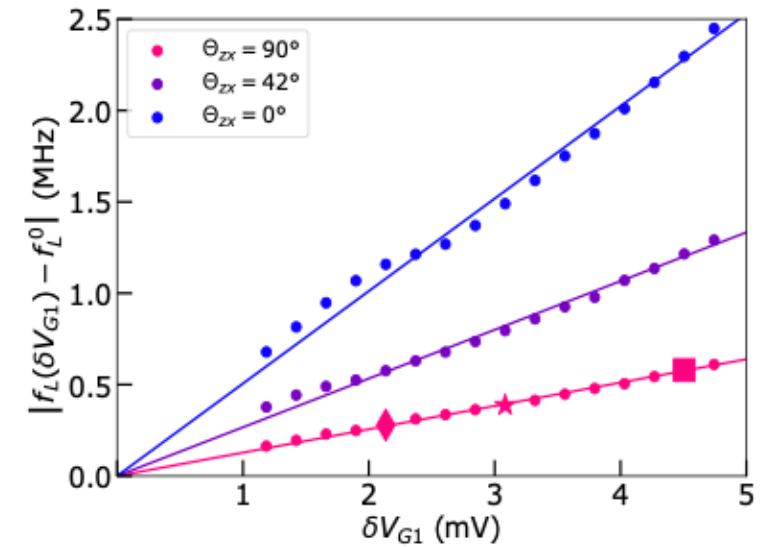
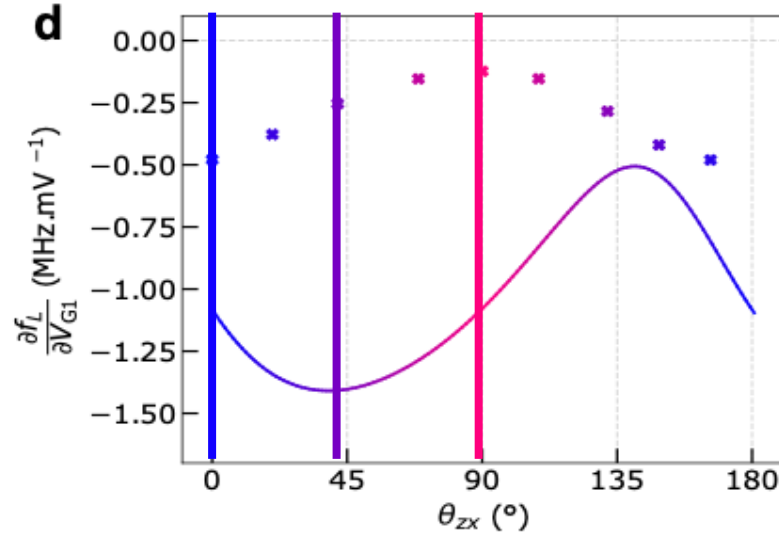
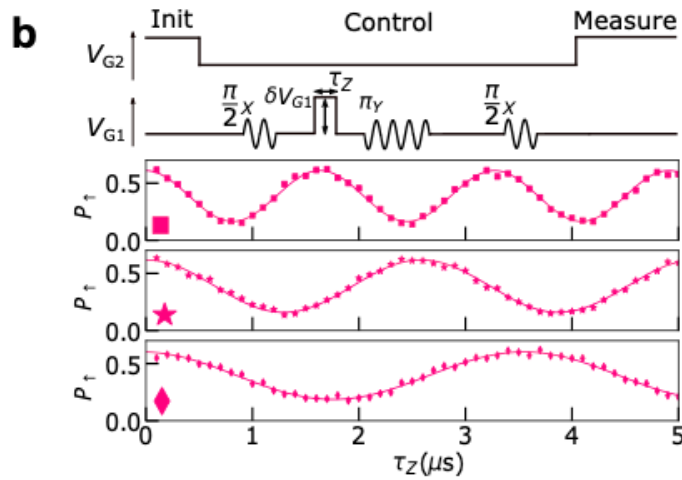
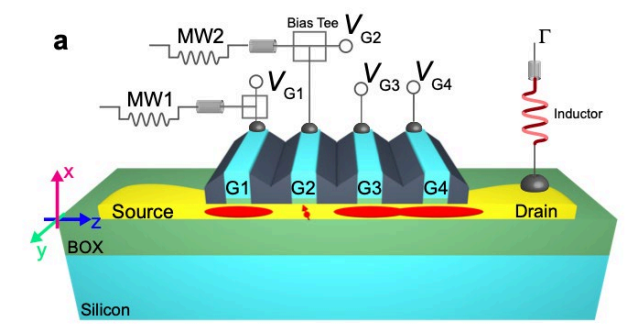
LSES of gate 2 (vertical) (fig. 2a / S6)

- Probe Chevron while applying gate voltage pulse to G2
- Rabi frequency clearly varying
- Measure df/dV for different angles in ZX plane

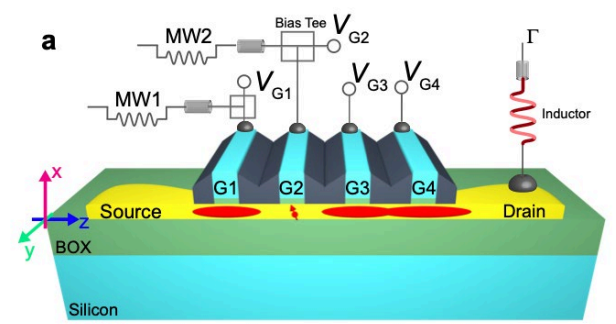


LSES of gate 1 ('horizontal') (fig. 2bcd)

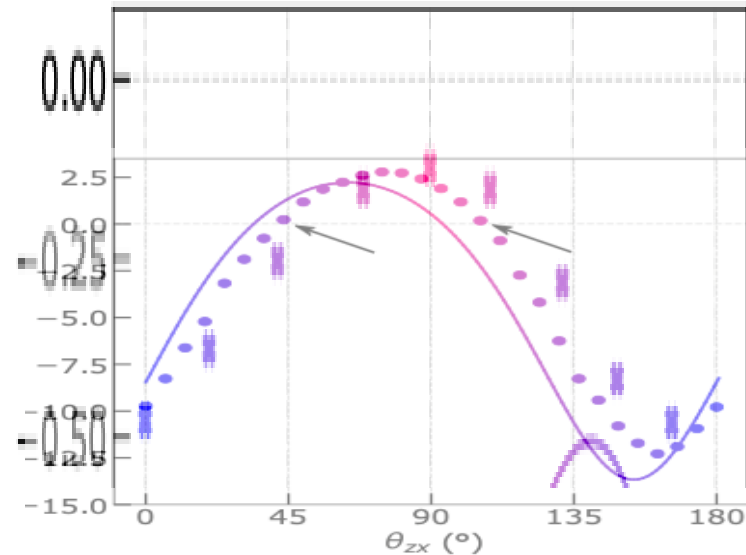
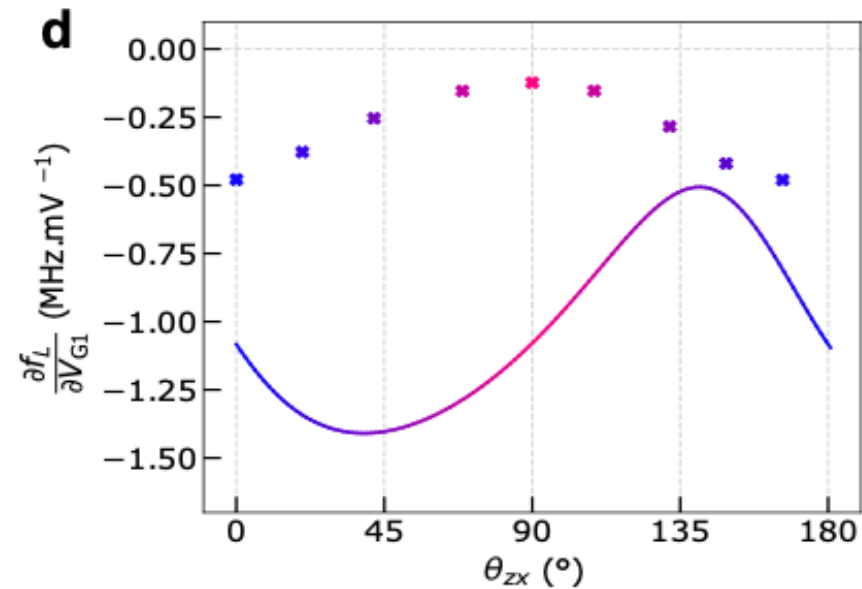
- Use Hahn echo to measure frequency shift
 - Unclear why the different methods for G1/G2
- No zero nodes for G1



LSES of gate 1 ('horizontal') (fig. 2)

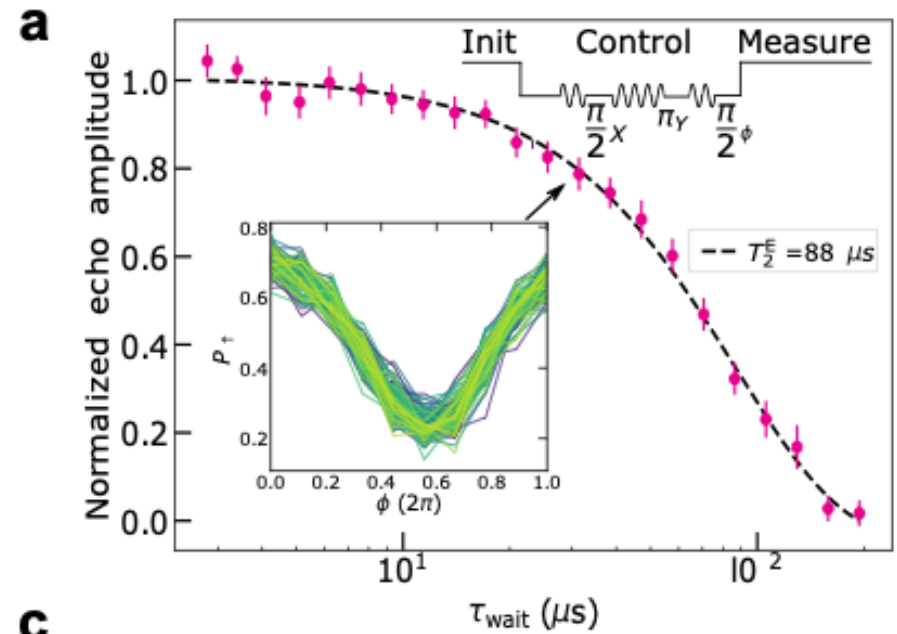
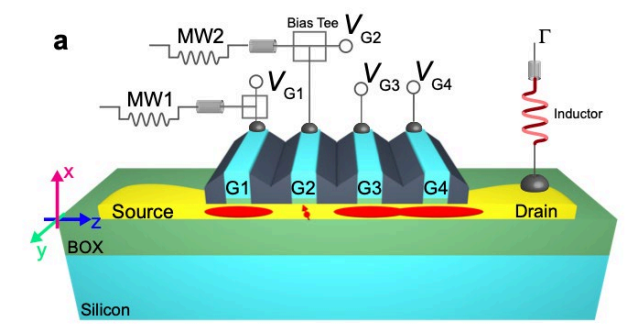


- Large discrepancy with the fit
 - They attribute this to charge disorder
- I wonder if this is a result of the horizontal/vertical assumption



Coherence times (fig. 3a)

- Measure Hahn coherence time to probe coherence
 - This eliminates low freq noise
 - $\exp\left(-\left(\frac{\tau_w}{T_2^E}\right)^\beta\right)$
 - $\beta = 1.5$, i.e. noise spectrum $S \propto \sqrt{f}$



c

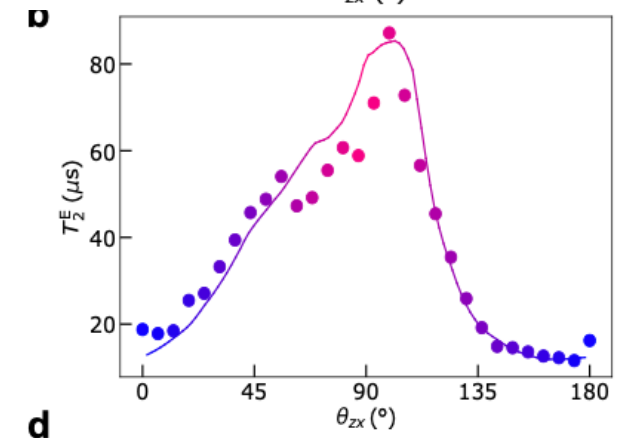
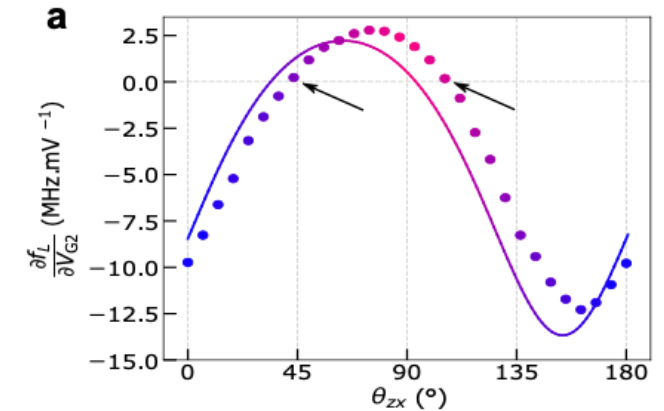
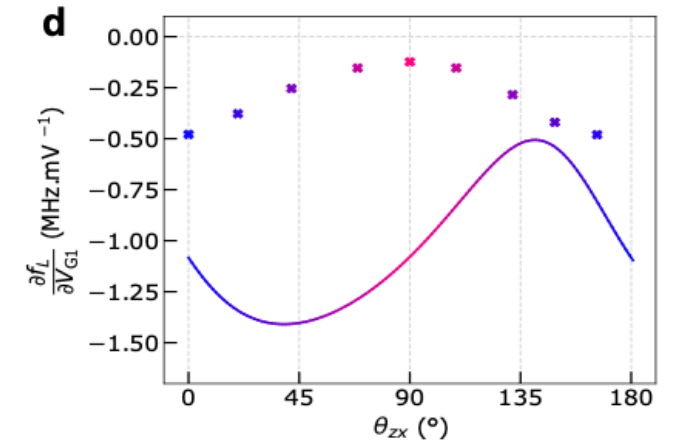
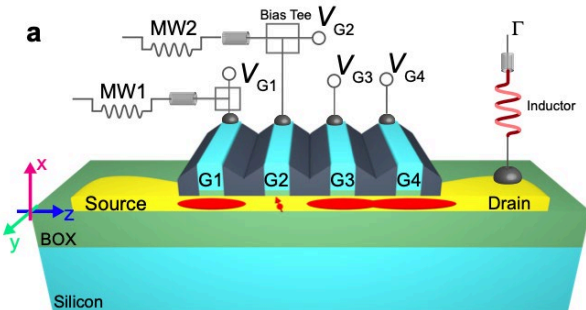
Coherence times (fig. 3b)

- Measure dependence on angle B in ZX plane
- Fit using obtained df/dV from before

$$\frac{1}{T_2^E} \approx 7.8 f_0^{1/3} \left(\sum_i \left(\frac{\partial f_L}{\partial V_{G_i}} \right)^2 S_{G_i}^{hf} \right)^{2/3}$$

← hf = high frequency, not hyperfine!

- Optimum near best points in G1 and G2



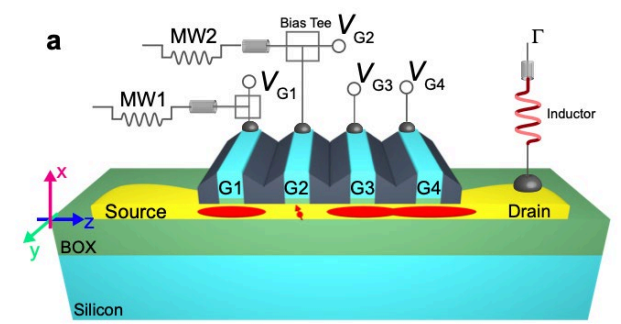
Coherence times

- Would there be much charge noise in z direction?
- Their fit:

$$\check{S}_{G1}^{\text{hf}} = (2.6 \mu\text{V} / \sqrt{\text{Hz}})^2$$

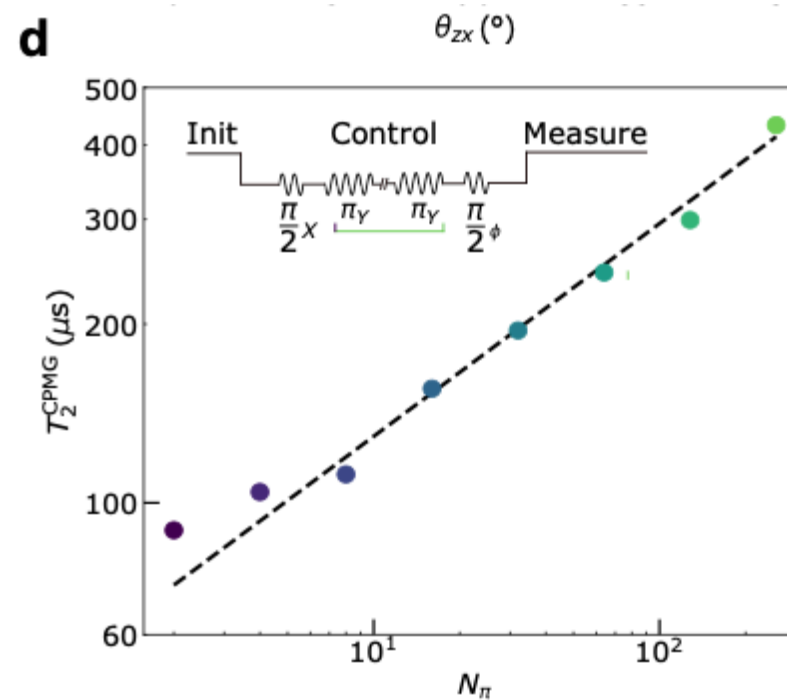
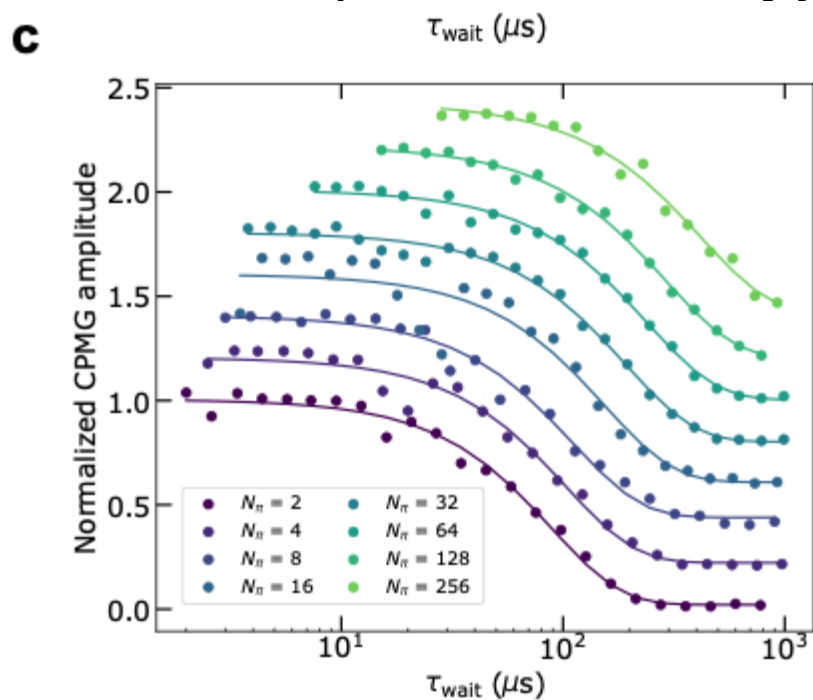
$$S_{G2}^{\text{hf}} = (0.1 \mu\text{V} / \sqrt{\text{Hz}})^2.$$

- Not much comment, but I find it highly unlikely...
 - (or the fins are really dirty)



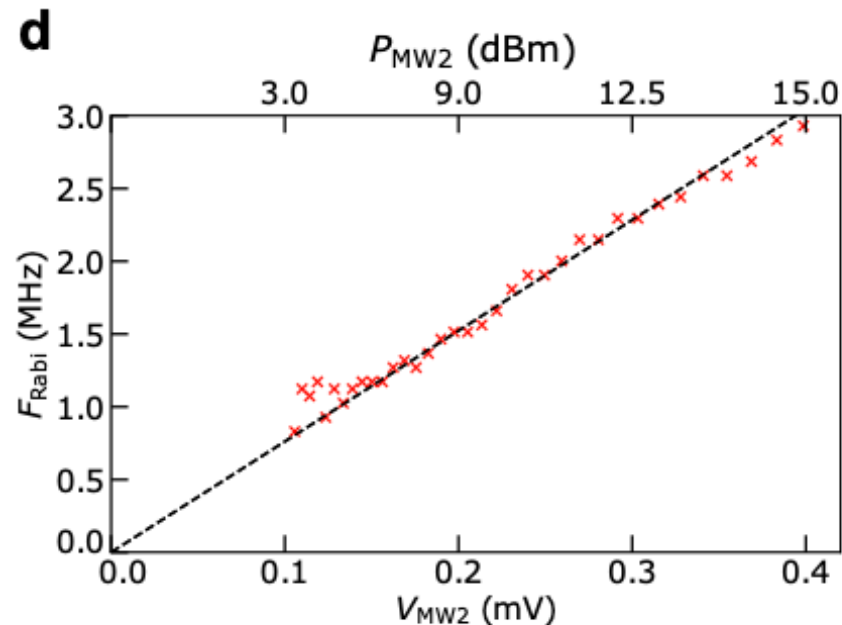
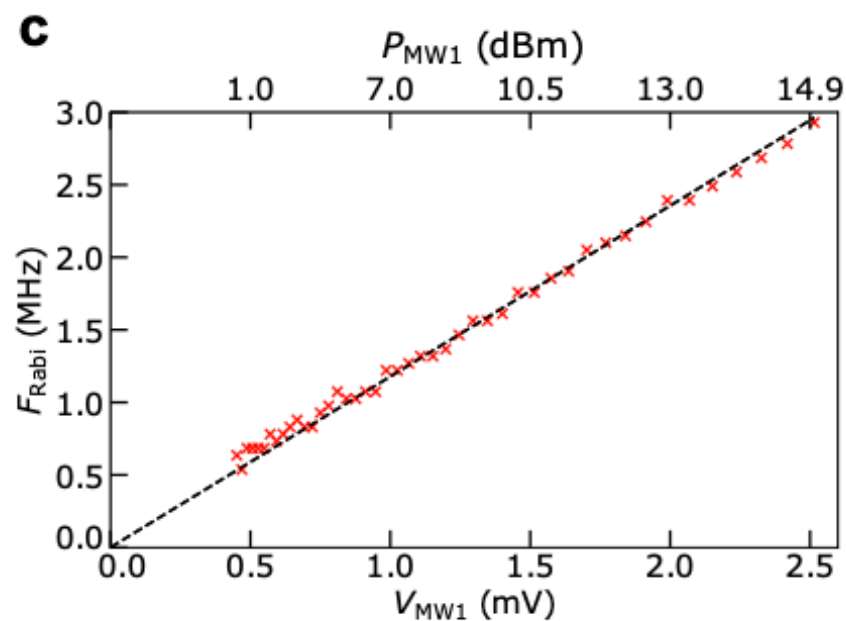
CPMG (fig. 3cd)

- Up to 400 us coherence
- Confirms noise spectrum $S \propto \sqrt{f}$



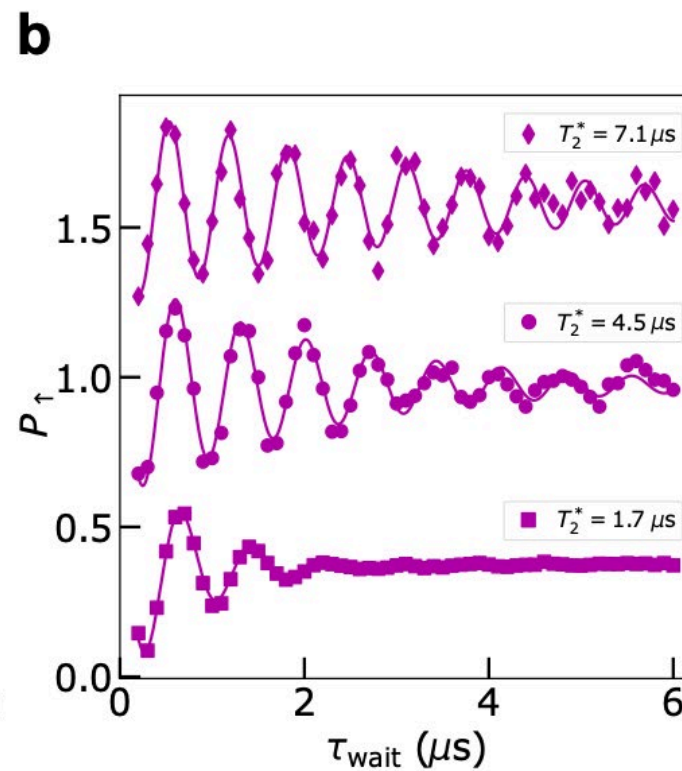
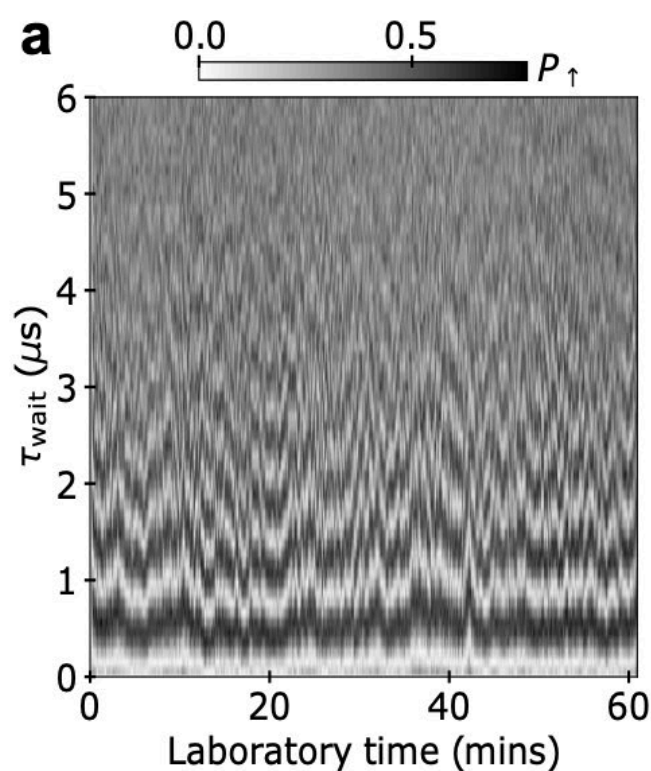
Driving (fig. S7cd)

- Driving possible for all field angles
- Rabi frequency changes, don't specify how much
- At the sweet spot max ~ 3 MHz, a lot stronger driving on G2.



T_2^* (fig 4ab)

- Measured (at sweet spot) as a function of integration time
 - Decreases for longer measurements, as expected



integration: 5.5 s (1 trace)

integration: 27.5 s (5 traces)

integration: 1 h (600 traces)

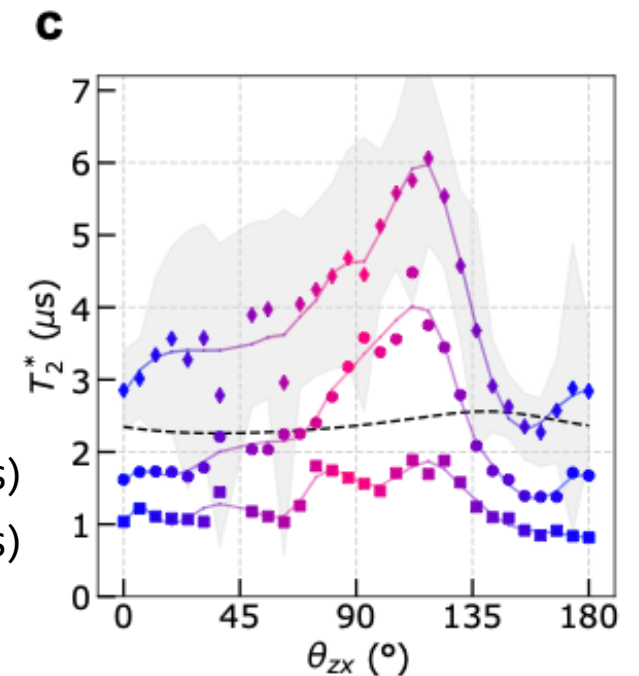
T_2^* (fig 4c)

- Angle dependence of T_2^*
- Deminishes for longer integration
 - Low freq noise is not dominated by charge noise
 - Supported by calculation of expected T_2^* for only the \sqrt{f} noise: ~ 50 μs .
 - Hyperfine?

integration: 5.5 s (1 trace)

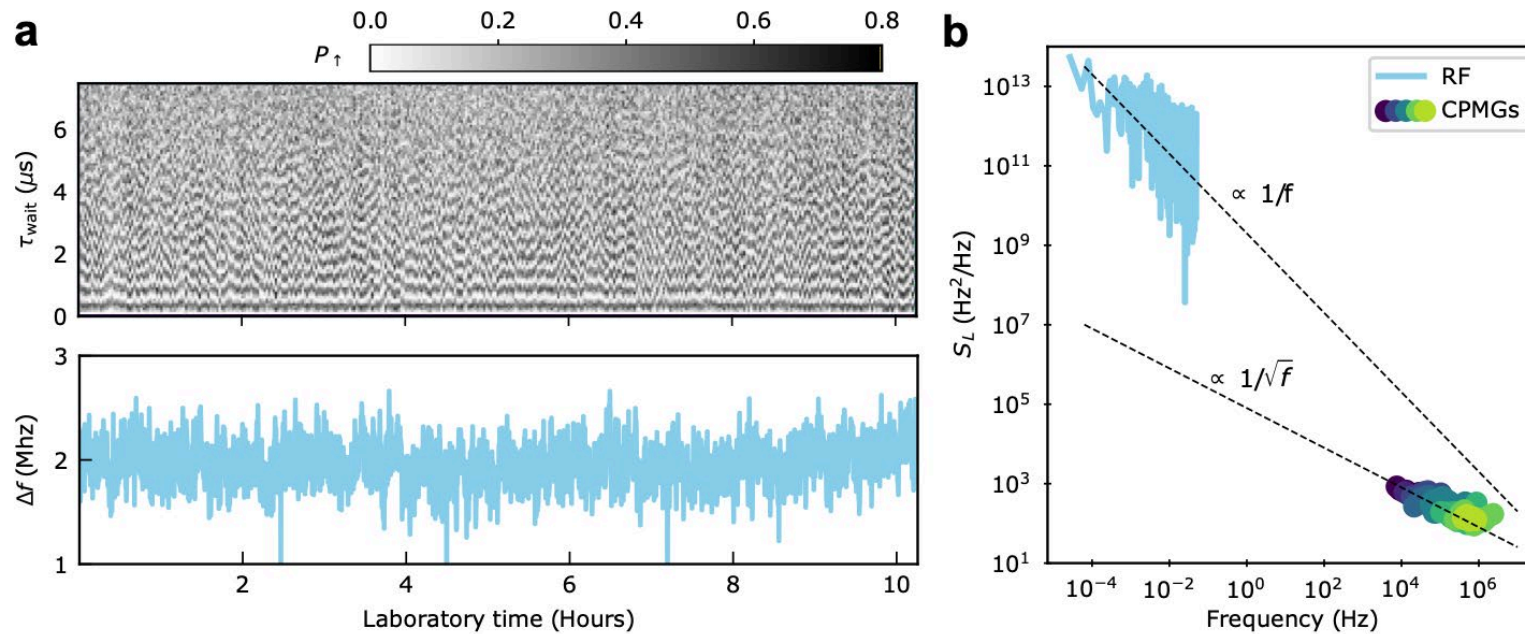
integration: 27.5 s (5 traces)

integration: 1 h (600 traces)



Noise spectrum (fig. S8)

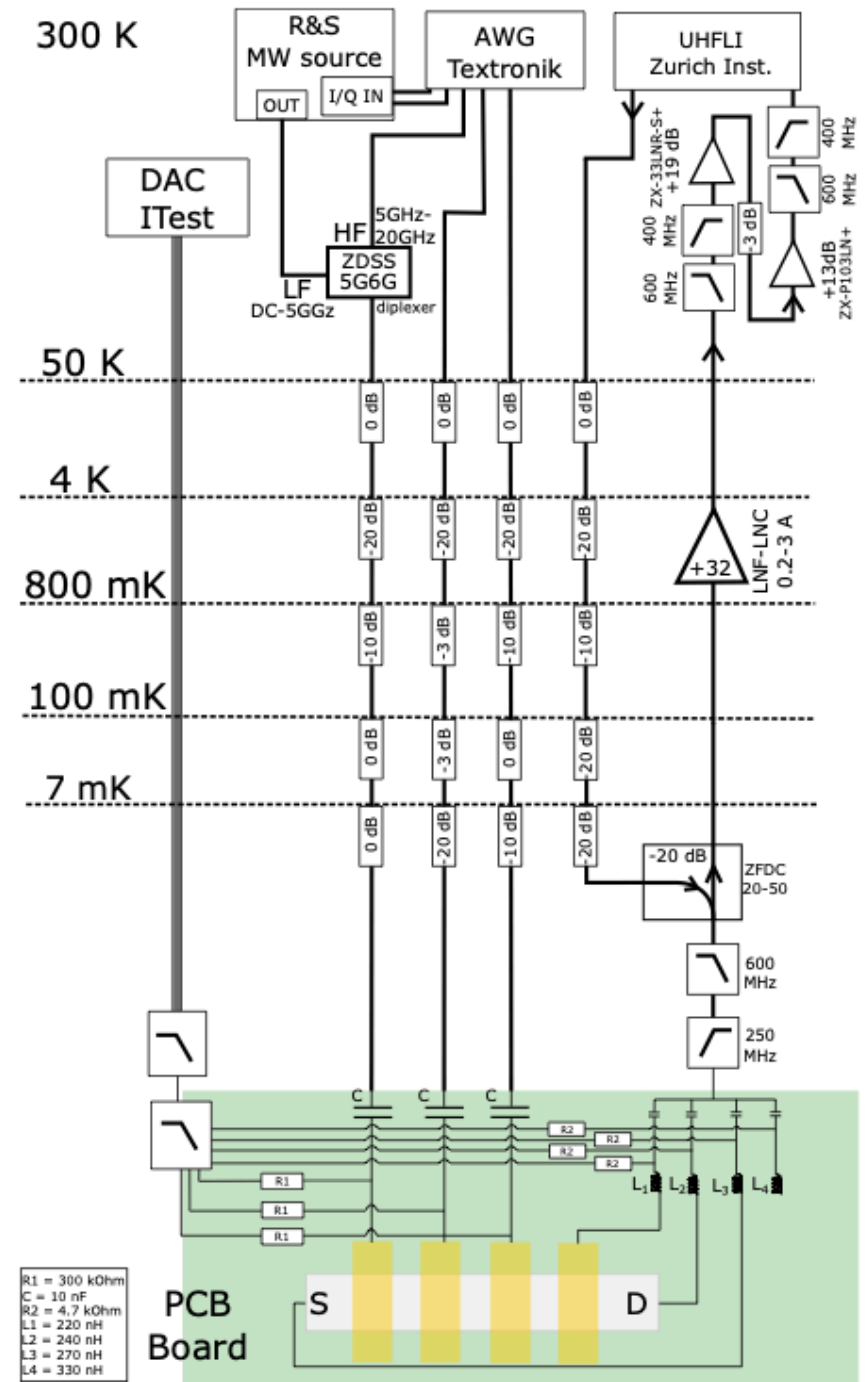
- CPMG: $S \propto \sqrt{f}$ at high freq
- FID: $S \propto f$ at low freq



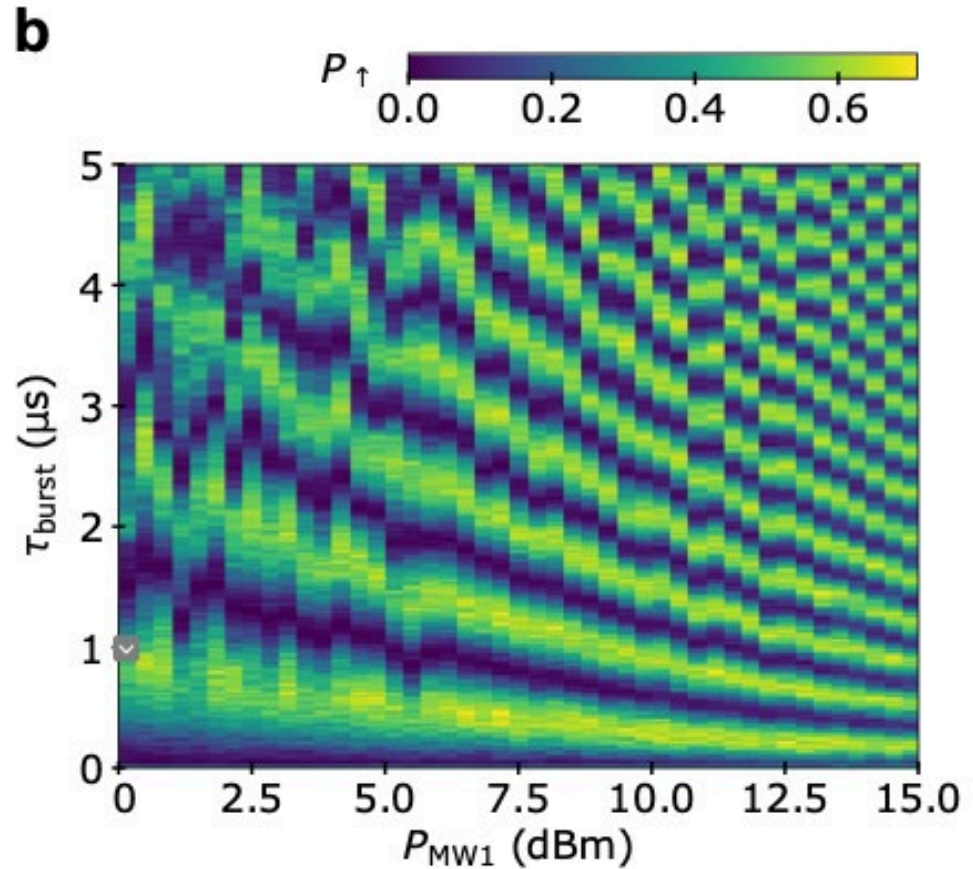
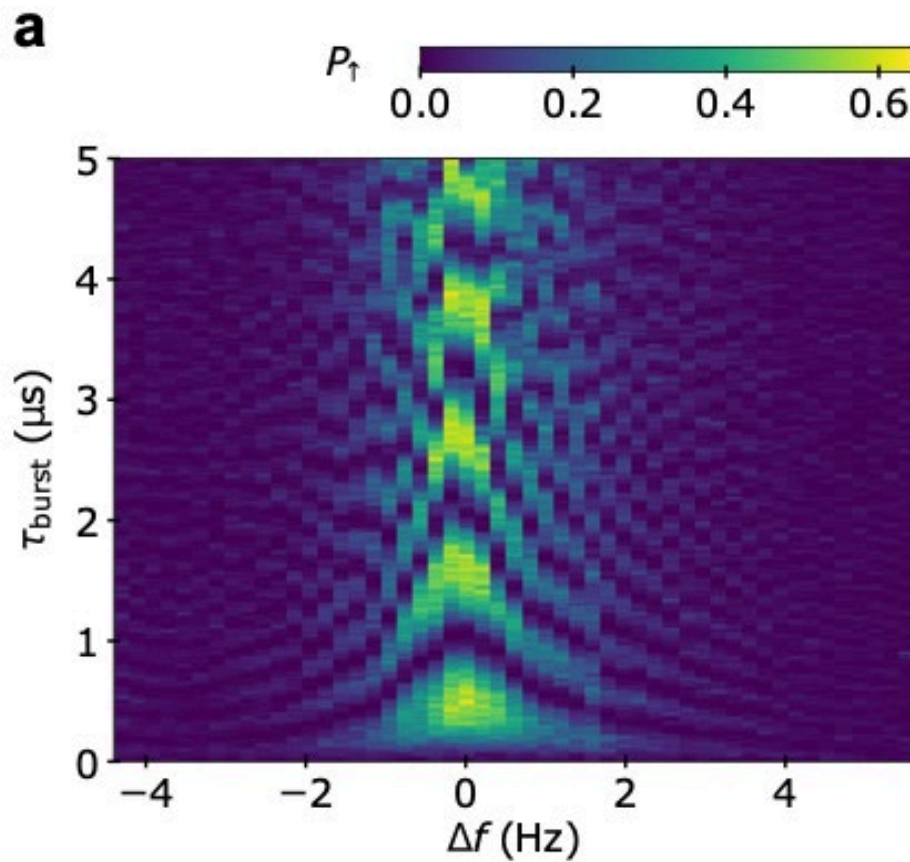
Conclusion

- Nice data, showing good promise for using sweet spots to increase hole coherence.
- I have some doubts with some of their fits/explanations
 - Many degrees of freedom and bold assumptions in my opinion.

Other figures: setup (fig. S9)



Other figures: chevron and power (fig. S7ab)



Other figures: different random charge arrangements (fig. S5b)

